Arabian Journal of Chemistry (2020) **13**, 7820–7828

King Saud University

Arabian Journal of Chemistry

www.ksu.edu.sa
www.sciencedirect.com

ORIGINAL ARTICLE

Eco friendly synthesis of the $LiY(MoO_4)_2$ coral-like quantum dots in biotemplate MOF (QD/BioMOF) for *in vivo* imaging and ibuprofen removal from an aqueous media study

Fahimeh Asadi [a], **Hamid Forootanfar** [b], **Mehdi Ranjbar** [b,c,*], **Ali Asadipour** [d]

[a] *Student Research Committee, Kerman University of Medical Sciences, Kerman, Iran*
[b] *Pharmaceutical Sciences and Cosmetic Products Research Center, Kerman University of Medical Sciences, Kerman, Iran*
[c] *Pharmaceutics Research Center, Institute of Neuropharmacology, Kerman University of Medical Sciences, Kerman, Iran*
[d] *Neuroscience Research Center, Institute of Neuropharmacology, Kerman University of Medical Sciences, Kerman, Iran*

Received 7 June 2020; accepted 8 September 2020
Available online 21 September 2020

KEYWORDS

$LiY(MoO_4)_2$ BQDMOFs;
Coral-Like;
Ibuprofen;
Hydrothermal Approach

Abstract Here as the first new research study on the bio quantum dots on metal–organic frameworks (BQDMOFs), we synthesized coral-like $LiY(MoO_4)_2$ BQDMOFs with hydrothermal method as an eco-friendly and cost effective approach. The lecithin as complex mixtures of lipids such as phospholipids which was extracted from egg yolk was applied not only as emulsifier for the formation of $LiY(MoO_4)_2$ quantum dots, but also acts as organic ligand and auxiliary linker agent on the base structure of the organic frameworks. The effect of such factors as pH (3–11), show with increasing pH from 3 up to 11 solubility increases and as a result the ibuprofen removal increases.The BQDMOFs structures were synthesized on the base of an organic frameworks with coral-like morphology with diameter in a range about 8–20 nm. The physicochemical properties, Ibuprofen removal from an aqueous media and *in vivo* imaging studies were investigated on the $LiY(MoO_4)_2$ BQDMOFs structures. Final products were characterization with analyze nanoparticle size using the well-known technique of dynamic light scattering (DLS), High-performance thin-layer chromatography (HPTLC), Powder X-ray diffraction (XRD), scanning electron microscopy (SEM), transmission electron microscopy (TEM), Infrared spectroscopy (IR) and the UV–Visible spectrum. From the sum of the results it can be established that $LiY(MoO_4)_2$ BQDMOFs structures acts not only as a super-radiant photoluminescence (SRP) substance for use in *in vivo* imaging in

* Corresponding author at: Pharmaceutical Sciences and Cosmetic Products Research Center, Kerman University of Medical Sciences, Kerman, Iran.
E-mail address: Mehdi.Ranjbar@kmu.ac.ir (M. Ranjbar).
Peer review under responsibility of King Saud University.

Production and hosting by Elsevier

https://doi.org/10.1016/j.arabjc.2020.09.013

small animal researches but also as a surface-specific material which can be use in removal of ibuprofen drug from an aqueous media. The photocatalyst results of the $LiY(MoO_4)_2$ BQDMOFs shows high removal efficiency of ibuprofen (more than 99%) after 60 min under the UV light.

1. 1.Introduction

Currently, nonsteroidal anti-inflammatory drugs (NSAIDs) such as ibuprofen, which used to treat mild and moderate pain have become popular among the people(Moore et al., 2015; Paul and Chauhan, 2005). Due to its many side effects such as biological and pharmacokinetic activity (Wang et al., 2018), it is important to remove and degradation of these drugs from aquatic environments (Liu et al., 2018). Nanostructures with their unique properties in morphological and chemical structure are capable to resolve various medical science challenges (Shukla et al., 2016; Matsuura and Rowlands, 2008). At the different stages of the drug production cycle also via veterinary practices, agriculture and aquaculture the contaminants enter the environment (Cole et al., 2011). Pharmaceutical agent's contaminants are one of the concerns that have attracted the attention of more and more researchers (Liu and Wong, 2013). There are many ways to remove pollutions of the pharmaceutical industry (Rivera-Utrilla et al., 2013; Collado et al., 2014; Quesada et al., 2019); The great advantage of using nanomaterials is that with a little amount of nanomaterial, more amount of the drug removed from the aquatic environment (Khan et al., 2017; Faraji and Wipf, 2009). The Ibuprofen [2-(4-(2-methyl propyl) phenyl] - propionic acid (molecular formula $C_{13}H_{18}O_2$) as a non-steroidal anti-inflammatory drug (Gonzalez-Rey and Bebianno, 2011), dissolved in wastewater in high concentration (Lin and Gan, 2011). Hence various techniques such as photo transformation sonolysis (Hapeshi et al., 2013), ultrasonic coagulation (Khmelev et al., 2013), with different types of nanomaterials (Fong et al., 2015) and sedimentation process (Zhao et al., 2000) have been employed to remove these contaminants from the environment. Nowadays nanotechnology, specially nanomaterials widely used in different fields such as biomedicine for the development *in vivo* imaging study (Peng and Chiu, 2015), drug delivery systems (Wen et al., 2017) and removal of pollutants (Taka et al., 2017). There are many literature reviews on the removal of ibuprofen by innovative techniques (Iovino et al., 2016a, 2016b; Hartmann et al., 2012; Peng et al., 2017). The metal-organic frameworks (MOFs) as a class of hybrid nonporous materials with two or three-dimensional structures are compounds consisting of metal ions which coordinated to organic ligands (Zhai et al., 2017). The MOFs compounds have unique characteristics and functionalities such as structural diversity (Khan et al., 2013), high surface area (Rangnekar et al., 2015), regular cavities (Gangu et al., 2016), high porosity, low density, high thermal and chemical stability (Zhou et al., 2018), crystallinity, adjustable topography and storage capacity which leading to extensive applications in different fields specially in the biomedical for efficient drug loading and delivery (Zhao et al., 2016), luminescence, absorption and separation in chemical processes (Hinks et al., 2010). The metal quantum dots (QDs) are a class of nanoparticles with a size of 2–10 nm, which absorb the light of one particular wavelength and convert it to another wavelength (Geszke-Moritz and Moritz, 2013; Zheng et al., 2007). Due to their high surface-to-volume ratio and their unique optical properties, they have many applications in intelligent medicine (Yildiz et al., 2011). The Bio-MOF are as a new strategy of the metal–organic frameworks structures which biomolecules are used as a coordinated ligands or the homogeneous metal phase coupling agent (Chianese et al., 2017; Gao et al., 2020; Iovino et al., 2019; Novakovic et al., 2020). Egg yolk as a rich source of lecithin agent was used in this study, lecithin as an unsaturated fat (without cholesterol) is chemically included in the phospholipid group and in this study was used as suitable emulsifier agent and also as an organic ligand agent to the formation of base structure of the organic frameworks (Sreedevi et al., 2012). In this work, the strategy of preparation of the Bio-QDMOFs nanostructures using lecithin as a biological ligand with hydrothermal approach as an ecofriendly method for the preparation of coral-like QDMOFs was investigated for the first time. The Bio-QMOFs after characterization of physico-chemical properties were evaluated for *in vivo* imaging study and removal of ibuprofen drug from an aqueous media. Summary of researches about Bio-MOFs applications in medical sciences has been reviewed in Table1.

2. 2.Experimental

2.1. Materials and apparatus

In this study, all the materials used were purified and used in standard conditions. Li_2SO_4 (Lithium sulfate %99), Potassium permanganate ($KMnO_4$ 7722–64-7, ≥99%) and Yttrium(III) nitrate hexahydrate (CAS Number 13494–98-9, ≥99%) were purchased from Merck company, the egg yolk used as lecithin ($C_{46}H_{89}NO_8P^{\pm}$) source. The pure ibuprofen ($C_{13}H_{18}O_2$) powders with a purity of over 99% were purchased from Alibaba company. 1,3,5-Benzenetricarboxylic acid 98% was purchased from Sigma-Aldrich through their representation in Iran. X-ray diffractometer using Ni-filtered Cu Kα radiation (X-ray diffraction patterns), Philips- X' Pert Pro, was used for crystallographic properties, miller indices and phase studies of the final products. The morphological and particle size distribution properties were performed with scanning electron microscopy (SEM- Philips XL-30 ESEM equipped with an energy dispersive X-ray spectroscopy (EDX) under the acceleration voltage of 100 kV. Hydrodynamic diameter of particle size was determined with Zeta-Sizer instrument, DLS, Malvern Zatasizer Nano-ZS, Worcestershire, UK. Fourier transform infrared (FT-IR) Shimadzu Varian 4300 spectrophotometer in KBr pellets used to identify functional groups. Digital pH Meter model Metrum pH-705 3 1/2 Digit , Large LCD Display, Max Display +/- 1999 was used in this study.

Table 1 Summary of researches about Bio-MOFs applications in medical sciences.

Types of Nanocomposites	Characterization	Synthesis method	Application	References
ZnO NPs	XRD, FT-IR,SEM, TEM	coprecipitation	bioactive curcumin	Su et al. (2015)
bio-MOF-12	XRD, FT-IR,Uv–vis	molecular simulations	CO_2/CH_4 separations	Erucar and Keskin (2015),
Fe3O4@bio-MOF	XRD, FT-IR,BET	sonochemical	efficient anti-leishmanial	Abazari et al. (2018)
bio-MOF-cobalt argeninate	HPLC,PXRD,TGA	chemical method	drug adsorption	, Sattar and Athar (2018), Sattar and Athar (2017)
Bio-MOF-29	PXRD, HPLC, TGA	hydrothermal	in Vitro Drugs Adsorption Studies	Sattar and Athar (2017)

Thermogravimetric-differential thermal analysis (TG-DTA) to evaluate the thermal stability of the specimens performed with a thermal gravimetric analysis instrument (Shimadzu TGA-50H) under a flow rate of 10.0 mL min^{-1}. The optical and the desired absorption concentrations were studied by a UV–Vis spectrophotometer (Shimadzu, UV-2550, Japan). For investigation of the separation of materials with higher sensitivity, accuracy and flexibility we used the high-performance thin-layer chromatography (HPTLC) technique CAMAG-Switzerland/ with measurement accuracy 10 $^{-5}$ Pg/ppb. Experimental studies for ibuprofen measurement in this study were including various detection methods such as ultraviolet spectrophotometric and high-performance liquid chromatography (HPLC). In this study also, the Effect of pH on ibuprofen removal have been investigated from 3 up to 11 in the aqueous media with the UV wavelength 222.5 nm in the concentration of 1000 ppm ibuprofen.

2.2. Preparation of Li_2MoO_4 in bio template

To the synthesis of the $LiY(MoO_4)_2$ BQDMOF in the first 0.04 g of Li_2SO_4 powder and 0.005 g $KMnO_4$ were dissolved in 20 mL distilled water under 50 °c and 500 rpm stirring for 30 min. Then different concentrations of egg yolk dropped in 5 mL H_2O and take place on shaker for 30 min. Both solutions were mixed in reflux system under 50 °C and 400 rpm for 45 min. The white precipitate phase collected with separator funnel.

2.3. Prepration of Coral-Like $LiY(MoO_4)_2$ BQDMOF

At this stage the 0. 2 g Li_2MoO_4 from the previous step and 0.01 g $Y(NO_3)_3{\cdot}6H_2O$ were primarily dissolved in 20 mL distilled water by continuous stirring 400 rpm at 60 ∘C. Then according to Table2 different concentrations of 1,3,5-Benzenetricarboxylic acid added to the solution until reaching pH up to the 7.3–8.4 (pH was adjusted with NaOH and HCl stock solution). Finally, the solution was transferred into Teflon lined stainless autoclave at 150 °C, 180 °C and 200 °C for 4 h 6 h and 8 h, the brown- dark precipitates were centrifuged in 5000 rpm and washed by distilled water and dried in autoclave for 48 h in 60 °C.

2.4. Ibuprofen removal

To investigate the elimination of ibuprofen, 2.2 mL of ibuprofen stock with 1000 ppm concentration was poured into the beaker glass, then 1.3 mL of 750 ppm stock of $LiY(MoO_4)_2$ QD/BioMOFs was added to above solution and every 15 min sampling was done at one hour. For each one mL of the sample which was removed and one mL of distilled water replaced.

2.5. HPTLC method

In this study, a silica gel plate 10 cm × 20 cm with a drop of 60-μm silica gel (Merck Germany) was used for the evaluation of HPTLC as method for the determination of $LiY(MoO_4)_2$ QD/BioMOFs samples. The specimens were then implanted on a plate by an autosampler (linear) and then developed in the extension module by a 9: 1 ratio of ethanol-distilled water solution for 45 min. Finally, the plate was analyzed by densitometry after drying inside the scanner at a wavelength of 254 nm at 5 cm / s and the resulting graphs were obtained.

2.6. In vivo imaging study

For investigate of *in vivo* imaging, 0.001 mg/mL of QDs dissolved at 1:2 ratios of three-times distilled water to ethanol and sonicated in an ultrasonic bath in 60 W for 15 min and then immediately injected to the left leg muscle of Balb/c male. Then 1:2 ratios of ketamine/xylazine for anesthesia was injected immediately, after 2 min' capture was did with kodak in-vivo imaging system F Pro. In vivo imaging This study received ethical approval (97000588) from the local ethical committee of the Kerman University of Medical Sciences. Male Balb/c weighing 150–200 g was fed with standard diet and kept under 12:12 hr light/dark cycles, at 20℃ and relative humidity of 25–30%.

3. Results and discussion

The arsanilic acid derivatives which were used as the specific nanocarriers for the affinity purification of alkaline phosphatase from the hen's egg yolk [1 1 1]. The hen's egg yolk Alkaline phosphatase (ALP) as a metalloprotein composed of two identical inactive subunits help effectively to form nanostructures. The ALP hydrolyzes phosphomonoester non-specific compounds at alkaline pH. To investigation of the influence of the different parameters such as the reaction time, temperature, pH, precursors concentration on morphological properties, properties of surface and the particle size distribution of the $LiY(MoO_4)_2$ BQDMOFs scanning electron

Table 2 Experimental conditions for the preparation of $LiY(MoO_4)_2$ QD/BioMOFs.

Sample	1,3,5 BTA (g)	pH	Egg yolk (mL)	Time(min)	Temp. (°C)	Morphology
S1	0.05	7.3–8.4	1	8	150	Coral-Like
S2	0.03	7.3–8.4	0.5	6	180	Coral-Like
S3	0.01	7.3–8.4	0.25	4	200	Coral-Like
S4	0.05	7.3–8.4	1	8	150	Coral-Like + particles
S5	0.03	7.3–8.4	0.5	6	180	Coral-Like + particles
S6	0.01	7.3–8.4	0.25	4	200	Needle-shaped leaves + particles
S7	0.05	7.3–8.4	1	8	150	Needle-shaped leaves + particles
S8	0.03	7.3–8.4	0.5	6	180	Coral-Like + particles
S9	0.01	7.3–8.4	0.25	4	200	Coral-Like + particles

microscope (SEM) applied. Fig. 1a-f shows the SEM images of the sample, S1, S3, S4, S6, S7 and S9 respectively. These images approve at high concentrations of lecithin (1 mL) and low temperature at hydrothermal process (150 °C) mono disperse $LiY(MoO_4)_2$ quantum dots have been supported on the metal–organic frameworks with unique morphology such as coral-like and needle-shaped leaves stained with nanoparticles are formed. With increasing reaction time and temperature due to increase in growth and nucleation of the $LiY(MoO_4)_2$ quantum dots, SEM images of samples show aggregated particles on MOFs structures. On the other hand, it can be predicted lecithin as a bio templet leads to uniform dispersion of metal cores in the formation of coral-Like MOFs structures.

Fig. 2a and b shows TEM image of MOFs structures without and with $LiY(MoO_4)_2$ quantum dots respectively. The observations show $LiY(MoO_4)_2$ quantum dots supported on the metal–organic frameworks in a way regular spherical uniformly. The average size and morphology observed from TEM was in good agreement with SEM images.

X-ray diffraction technique as a non-destructive and useful characterization tool was utilized to study structural information, chemical composition, crystallite size and the crystallographic properties. Fig. 3a shows the XRD pattern of $LiY(MoO_4)_2$ quantum dots structures. The XRD results indicated there are many intensity and strong sharp peaks in the pattern which approved the obtained quantum dots structures are well crystallized. The presence of noise peaks is due to the existence of the organic compounds such as 1,3,5-Benzenetricarboxylic acid and lecithin in final products. The peaks in XRD pattern can be indexed as hexagonal structure, also with a lattice constant a = 4.123 °A (JCPDS No. 00–017-0773). The crystallite sizes of the $LiY(MoO_4)_2$ quantum dots structures were calculated by Scherrer equation, $D_c = K\lambda/\beta\cos\theta$ where, k is as shape factor (about 0.9), λ and β are the wavelength of the X-ray source and the breadth of the widest peak at its half intensity maximum. According to the calculations, the particle size was approximately 20 nm. Particle size distribution of the MOFs supported with $LiY(MoO_4)_2$ quantum dots structures display in Fig. 3b. The hydrodynamic radius of a diffusing sphere can be calculated via the Stokes-Einstein equation:

$$rh = k.\frac{T}{6}.n.\pi.D \quad (1)$$

where k is Boltzmann's constant, T is the temperature in K, D is diffusion coefficient and n is the solvent viscosity. The existence of the MOFs as a support platform for the $LiY(MoO_4)_2$ quantum dots structures leads to create distribution number 90% with very fine sizes in range about 11.17 nm.

Thermogravimetric analysis (TGA) as a technique which calculate the mass of a specimen as a function of temperature or time in a controlled atmosphere. Fig. 4a illustrates the TGA and Differential thermal analysis (DTG) curve of the $LiY(MoO_4)_2$ quantum dots supported on the metal-organic frameworks under nitrogen atmosphere at the temperature ranging from 50 to 350 °C. TGA and DTG graphs of the $LiY(MoO_4)_2$ QD/BioMOFs demonstrate a continuous decomposition stage which can indicate structural stability. At first, with a little slope, the water in the structure is lost, subsequently, by the loss of intermolecular bonds in BioMOFs, the product will be destroyed in about 350 °C completely, the presence of strong covalent bonds causes the temperature stability of the structure. Fourier-transform infrared spectroscopy (FT-IR) used as a qualitative method for identify the functional groups in the structure of a species. Fig. 4b and 4c indicates the infrared spectrum of Li_2MoO_4 and $LiY(MoO_4)_2$ QD/BioMOFs in the region 400–4000 cm^{-1} respectively. The absorption peak at about 3254 cm^{-1} can be corresponding to O-H trapped in structure. The absorption peaks at 2850 cm^{-1} and 1450 cm^{-1} are corresponding to CH_2, C—OH and C═O stretching band in lecithin as biotemplate structure for the formation of Li_2MoO_4. The absorption bands observed at 970–500 cm^{-1} are related to Li—O vibrations, and the individual MoO_4^{2-} ions (Sobeih et al., 2020, El-Berry et al,. 2020). The presence of organic structures such as 1,3,5-Benzenetricarboxylic acid and carbon chains in lecithin structure leads to creating noise peaks in FT-IR spectrum of the $LiY(MoO_4)_2$ QD/BioMOFs in Fig. 4c.

The investigation of ibuprofen removal from an aqueous media was evaluated with UV–Vis spectrophotometer. According to literature review, an absorption wavelength ranges between 200 nm and 280 nm selected (Li et al., 2015) for ibuprofen removal from an aqueous media. Finally, the absorbance obtained at 222.5 nm were used for the calculation of the equation of a straight line as y = 0.3258x-0 0938 with R^2 = 0.9995. Initially, the highest removal rate occurs because the sample concentration (catalyst) is at its highest. From the beginning of time (zero) until 60 min further final concentration (CF) changes from 8.22 ppm to 2.90 ppm and it can be seen in 60 min after the start ibuprofen removal from an aqueous media with $LiY(MoO_4)_2$ QD/BioMOFs happens about

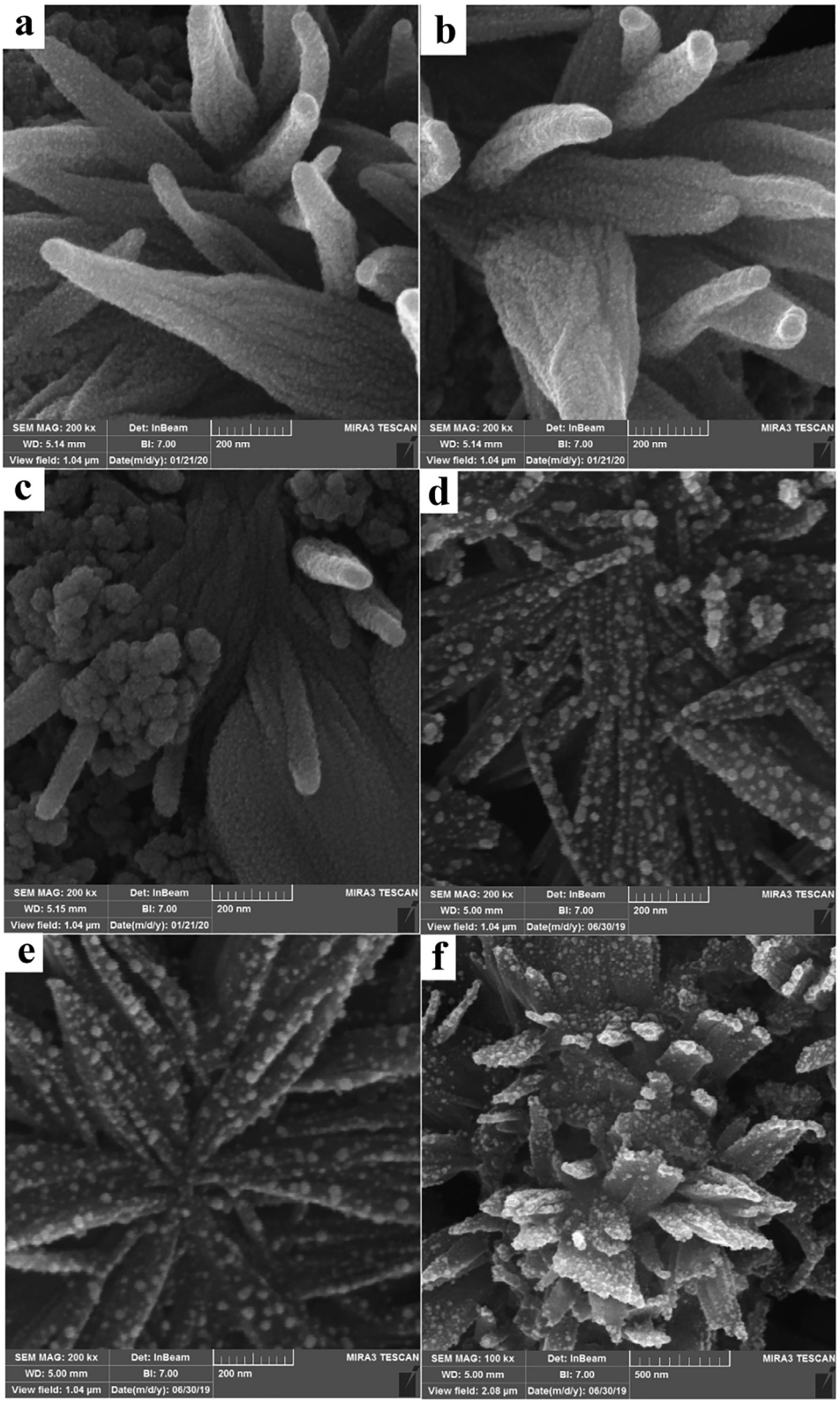

Fig. 1 The SEM images of the sample, S1 (a), S3 (b), S4 (c), S6 (d), S7 (e) and S9 (f).

99.70%. Fig. 5(a)–(d) show curve of effect time on the wavelength absorption graph, curve of percentage removal of ibuprofen relative to time and calibration curve for the calculation of the equation of a straight line and effect of pH on ibuprofen removal have been investigated from 3 up to 11 in the aqueous media respectively. The effect of such factors as pH (Wang et al., 2018; Liu et al., 2018; Shukla et al., 2016; Matsuura and Rowlands, 2008; Cole et al., 2011; Liu and

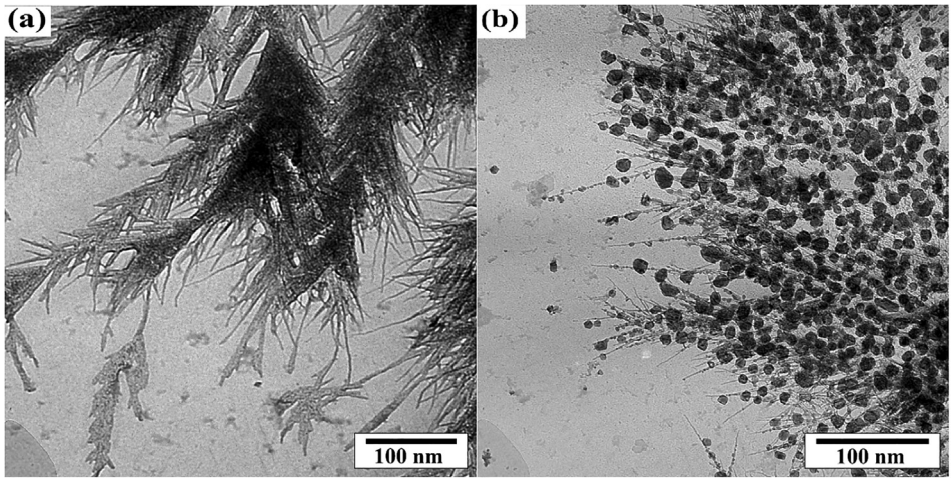

Fig. 2 TEM image of MOFs structures without (a) and with $LiY(MoO_4)_2$ quantum dots (b).

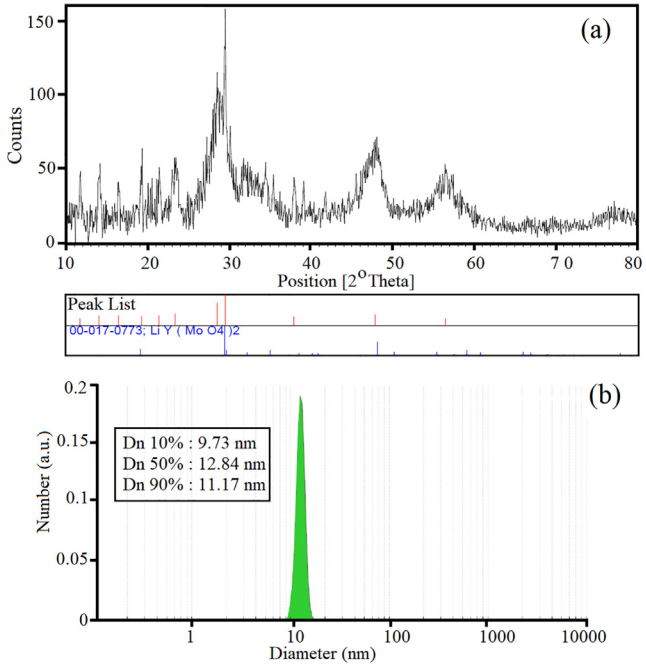

Fig. 3 The XRD pattern of $LiY(MoO_4)_2$ quantum dots (a), DLS diagram of particle size distribution of the MOFs supported with $LiY(MoO_4)_2$ quantum dots structures.

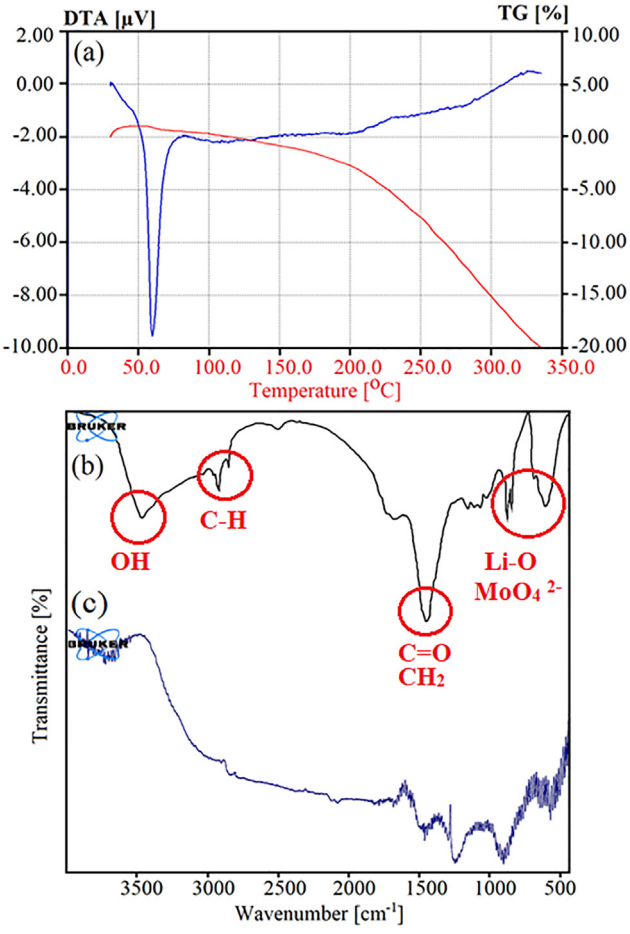

Fig. 4 TGA and DTG curve of the $LiY(MoO_4)_2$ quantum dots supported on the metal–organic frameworks under nitrogen atmosphere (a), infrared spectrum of Li_2MoO_4 (b) and $LiY(MoO_4)_2$ QD/BioMOFs (c) in the region 400–4000 cm^{-1}.

Wong, 2013; Rivera-Utrilla et al., 2013; Collado et al., 2014; Quesada et al., 2019), show with increasing pH from 3 up to 11 solubility increases and as a result the ibuprofen removal increases. The results of photocatalytic adsorption of the ibuprofen have been reported in many research papers (Gu et al., 2019; Khan et al., 2019; Liu et al., 2019).

Fig. 6a and b show UV spectrum of $LiY(MoO_4)_2$ QD/Bio-MOFs related to sample 1 at different concentration and 3D diagram of HPTLC chromatogram of $LiY(MoO_4)_2$ QD/Bio-MOFs at 254 nm respectively. The results show that by decreasing the concentration from 1000 ppm to 6.25 ppm, we observe a blue shift wavelength. This blue shift of the coral-like $LiY(MoO_4)_2$ QD/BioMOFs can be due to the quantum size effect, also decreasing band gap though smaller particle size in quantum dot nanoparticles. Retention Factor (Rf)

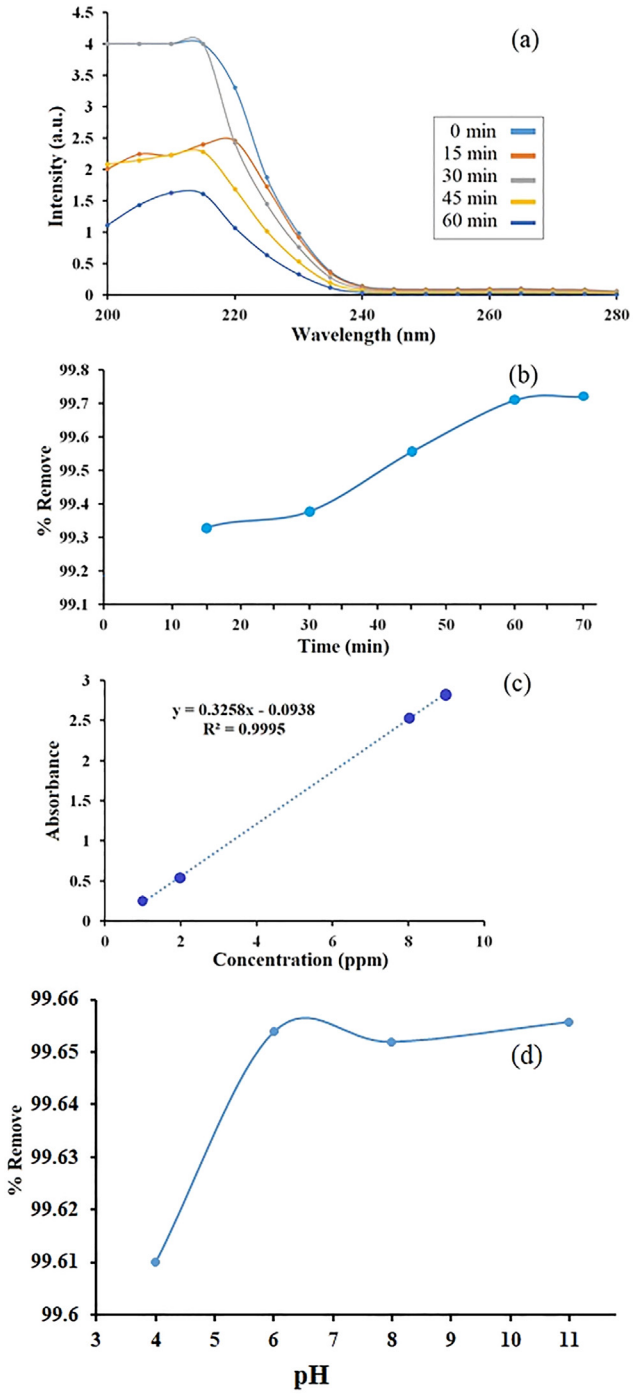

Fig. 5 Curve of effect time on the wavelength absorption graph (a), curve of percentage removal of ibuprofen relative to time (b) and calibration curve (c) and effect of pH on the ibuprofen removal (d).

as represented can show the location of each spot on the HPTLC and calculated according to the following equation:

$$Rf = a/b \tag{2}$$

While a function is the distance from the starting point to the center of the spot on the plate and b function is he distance from the starting point to the solvent front. The HPTLC chromatogram of $LiY(MoO_4)_2$ QD/BioMOFs at 254 nm show evidenced 2 spots with order of Rf values 0.00 and 0.93. Each track has two peaks whose first peak has zero retention factors

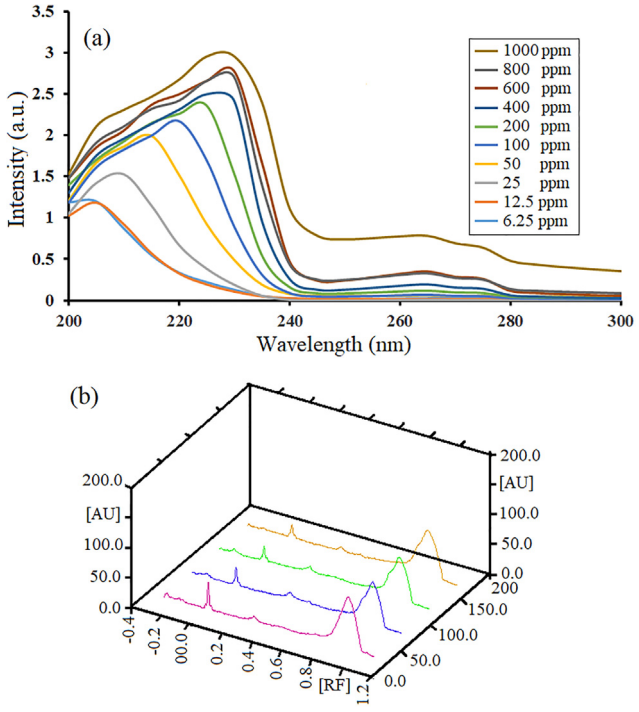

Fig. 6 Uv spectrum of $LiY(MoO_4)_2$ QD/BioMOFs related to sample 1 at different concentration (a) and 3D diagram of HPTLC chromatogram of $LiY(MoO_4)_2$ QD/BioMOFs at 254 nm (b).

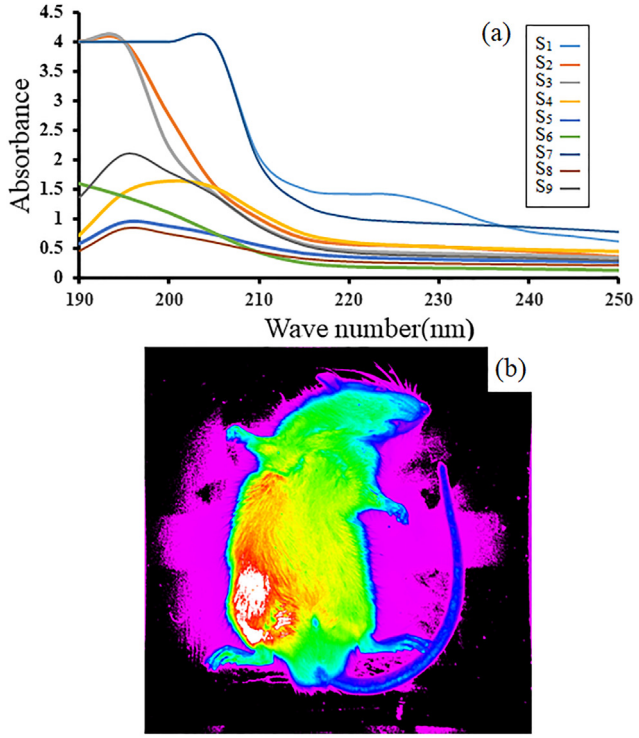

Fig. 7 The UV–vis absorption spectrum of the $LiY(MoO_4)_2$ QD/BioMOFs (a) and *in vivo* image study of sample1 in left leg muscle of mice 1 min after injection (b).

(Rf), because it's a sampling location and it doesn't move. The second peak whose Rf is about 0.9 is the main peak. With densitometry in UV–Vis range at 254 nm of HPTLC, it can be clearly seen that the presence of a peak indicates the biological species of lecithin in the egg yolk.

Fig. 7a and 7b illustrate the UV–vis absorption spectrum of the $LiY(MoO_4)_2$ QD/BioMOFs and *in vivo* image study of sample1 in left leg muscle of mice 1 min after injection respectively. To investigate the optical properties of $LiY(MoO_4)_2$ QD/BioMOFs all the samples analyzed with UV spectrum in range 200 nm-250 nm. The quantum dots due to the discrete band gap energy level have the frequency light emitted and major impact on the color. Results show an emission band centered at 195–208 nm for all samples and also increase in intensity of the UV spectrum can be related to $LiY(MoO_4)_2$ QD trapped in the BioMOFs which existence of this platform covers the surface of $LiY(MoO_4)_2$ QDs and protects it from the aggregation. Observe red-shift in the different samples can be related to originated from the recombination of charged oxygen vacancy in MoO_4^{2-}. The optical properties of coral-like $LiY(MoO_4)_2$ QD/BioMOFs shows that particles exhibit good optical properties in the living organism, therefore, these substances can be having a suitable strategy for carrying anticancer drugs.

4. Conclusions

In this experimental work $LiY(MoO_4)_2$ QD/BioMOFs were ecofriendly synthesis with hydrothermal method and used for ibuprofen removal from an aqueous media and *in vivo* imaging study. For the first time the lecithin extracted from egg yolk was applied not only as emulsifier for the formation of $LiY(MoO_4)_2$ quantum dots but also acts as a suitable auxiliary linker for the formation BioMOFs. Also it was fount which morphology of $LiY(MoO_4)_2$ QD/BioMOFs is completely unique coral-like. Final products were characterization with DLS, XRD, SEM, TEM, IR, UV–Visible spectrum and HPTLC. Results show that $LiY(MoO_4)_2$ BQDMOFs structures can activate as a super absorbent with high removal efficiency of ibuprofen (more than 99%) after 60 min under the UV light and also as a superradiant photoluminescence (SRP) substance for use in *in vivo* imaging which can make these materials suitable for drug delivery system in anti-cancer drugs.

Declaration of Competing Interest

The authors declare that they have no known competing financial interests or personal relationships that could have appeared to influence the work reported in this paper.

Acknowledgments

Authors are grateful to council of Pharmaceutical Sciences and Cosmetic Products Research Center, Kerman University of Medical Sciences, Kerman, Iran with grant number 98000804.

References

Moore, N., Pollack, C., Butkerait, P., 2015. Adverse drug reactions and drug–drug interactions with over-the-counter NSAIDs. Ther. Clin. Risk Manag. 11, 1061.

Paul, A., Chauhan, C., 2005. Study of usage pattern of nonsteroidal anti-inflammatory drugs (NSAIDs) among different practice categories in Indian clinical setting. Eur. J. Clin. Pharmacol. 60 (12), 889–892.

Wang, T-y, Li, Q., Bi, K-s, 2018. Bioactive flavonoids in medicinal plants: Structure, activity and biological fate. Asian J. Pharm. Sci. 13 (1), 12–23.

Liu, X., Lu, S., Guo, W., Xi, B., Wang, W., 2018. Antibiotics in the aquatic environments: a review of lakes, China. Sci. Total Environ. 627, 1195–1208.

Shukla, S., Shukla, S.K., Govender, P.P., Giri, N., 2016. Biodegradable polymeric nanostructures in therapeutic applications: opportunities and challenges. RSC Adv. 6 (97), 94325–94351.

Matsuura, N., Rowlands, J., 2008. Towards new functional nanostructures for medical imaging. Med. Phys. 35 (10), 4474–4487.

Cole, M., Lindeque, P., Halsband, C., Galloway, T.S., 2011. Microplastics as contaminants in the marine environment: a review. Mar. Pollut. Bull. 62 (12), 2588–2597.

Liu, J.-L., Wong, M.-H., 2013. Pharmaceuticals and personal care products (PPCPs): a review on environmental contamination in China. Environ. Int. 59, 208–224.

Rivera-Utrilla, J., Sánchez-Polo, M., Ferro-García, M.Á., Prados-Joya, G., Ocampo-Pérez, R., 2013. Pharmaceuticals as emerging contaminants and their removal from water. A review. Chemosphere 93 (7), 1268–1287.

Collado, N., Rodriguez-Mozaz, S., Gros, M., Rubirola, A., Barceló, D., Comas, J., et al, 2014. Pharmaceuticals occurrence in a WWTP with significant industrial contribution and its input into the river system. Environ. Pollut. 185, 202–212.

Quesada, H.B., Baptista, A.T.A., Cusioli, L.F., Seibert, D., de Oliveira, Bezerra C, Bergamasco, R., 2019. Surface water pollution by pharmaceuticals and an alternative of removal by low-cost adsorbents: A review. Chemosphere.

Khan, A., Wang, J., Li, J., Wang, X., Chen, Z., Alsaedi, A., et al, 2017. The role of graphene oxide and graphene oxide-based nanomaterials in the removal of pharmaceuticals from aqueous media: a review. Environ. Sci. Pollut. Res. 24 (9), 7938–7958.

Faraji, A.H., Wipf, P., 2009. Nanoparticles in cellular drug delivery. Bioorg. Med. Chem. 17 (8), 2950–2962.

Gonzalez-Rey, M., Bebianno, M.J., 2011. Non-steroidal anti-inflammatory drug (NSAID) ibuprofen distresses antioxidant defense system in mussel Mytilus galloprovincialis gills. Aquat. Toxicol. 105 (3–4), 264–269.

Lin, K., Gan, J., 2011. Sorption and degradation of wastewater-associated non-steroidal anti-inflammatory drugs and antibiotics in soils. Chemosphere 83 (3), 240–246.

Hapeshi, E., Fotiou, I., Fatta-Kassinos, D., 2013. Sonophotocatalytic treatment of ofloxacin in secondary treated effluent and elucidation of its transformation products. Chem. Eng. J. 224, 96–105.

Khmelev VN, Shalunov AV, Nesterov VA, Galakhov AN, Golykh RN, Khmelev MV, editors. The control of the ultrasonic coagulation of dispersed nanoscale particles. 2013 14th International Conference of Young Specialists on Micro/Nanotechnologies and Electron Devices; 2013: IEEE.

Fong, J.F.Y., Chin, S.F., Ng, S.M., 2015. Facile synthesis of carbon nanoparticles from sodium alginate via ultrasonic-assisted nanoprecipitation and thermal acid dehydration for ferric ion sensing. Sens. Actuat. B 209, 997–1004.

Zhao, W., Ting, Y., Chen, J., Xing, C., Shi, S., 2000. Advanced primary treatment of waste water using a bio-flocculation-adsorption sedimentation process. Acta Biotechnol. 20 (1), 53–64.

Peng, H.-S., Chiu, D.T., 2015. Soft fluorescent nanomaterials for biological and biomedical imaging. Chem. Soc. Rev. 44 (14), 4699–4722.

Wen, J., Yang, K., Liu, F., Li, H., Xu, Y., Sun, S., 2017. Diverse gatekeepers for mesoporous silica nanoparticle based drug delivery systems. Chem. Soc. Rev. 46 (19), 6024–6045.

Taka, A.L., Pillay, K., Mbianda, X.Y., 2017. Nanosponge cyclodextrin polyurethanes and their modification with nanomaterials for the removal of pollutants from waste water: A review. Carbohydr. Polym. 159, 94–107.
Iovino, P., Chianese, S., Canzano, S., Prisciandaro, M., Musmarra, D., 2016. Degradation of ibuprofen in aqueous solution with UV light: the effect of reactor volume and pH. Water Air Soil Pollut. 227 (6), 1–9.
Hartmann, A., Buhl, J.C., Lutz, W., 2012. Synthesis and properties of zeolites from autoclaved aerated concrete (AAC) waste. Zeitschrift für anorganische und allgemeine Chemie. 638 (9), 1297–1306.
Peng, M., Li, H., Kang, X., Du, E., Li, D., 2017. Photo-degradation ibuprofen by UV/H2O2 process: response surface analysis and degradation mechanism. Water Sci. Technol. 75 (12), 2935–2951.
Iovino, P., Chianese, S., Canzano, S., Prisciandaro, M., Musmarra, D., 2016. Ibuprofen photodegradation in aqueous solutions. Environ. Sci. Pollut. Res. 23 (22), 22993–23004.
Zhai, Q.-G., Bu, X., Zhao, X., Li, D.-S., Feng, P., 2017. Pore space partition in metal–organic frameworks. Acc. Chem. Res. 50 (2), 407–417.
Khan, N.A., Hasan, Z., Jhung, S.H., 2013. Adsorptive removal of hazardous materials using metal-organic frameworks (MOFs): a review. J. Hazard. Mater. 244, 444–456.
Rangnekar, N., Mittal, N., Elyassi, B., Caro, J., Tsapatsis, M., 2015. Zeolite membranes–a review and comparison with MOFs. Chem. Soc. Rev. 44 (20), 7128–7154.
Gangu, K.K., Maddila, S., Mukkamala, S.B., Jonnalagadda, S.B., 2016. A review on contemporary Metal-Organic Framework materials. Inorg. Chim. Acta 446, 61–74.
Zhou J, Tian G, Zeng L, Song X, Bian Xw. Nanoscaled Metal-Organic Frameworks for Biosensing, Imaging, and Cancer Therapy. Advanced healthcare materials. 2018;7(10):1800022.
Zhao, H.-X., Zou, Q., Sun, S.-K., Yu, C., Zhang, X., Li, R.-J., et al, 2016. Theranostic metal–organic framework core–shell composites for magnetic resonance imaging and drug delivery. Chem. Sci. 7 (8), 5294–5301.
Hinks, N.J., McKinlay, A.C., Xiao, B., Wheatley, P.S., Morris, R.E., 2010. Metal organic frameworks as NO delivery materials for biological applications. Micropor. Mesopor. Mater. 129 (3), 330–334.
Geszke-Moritz, M., Moritz, M., 2013. Quantum dots as versatile probes in medical sciences: synthesis, modification and properties. Mater. Sci. Eng. C 33 (3), 1008–1021.
Zheng, J., Nicovich, P.R., Dickson, R.M., 2007. Highly fluorescent noble-metal quantum dots. Ann. Rev. Phys. Chem. 58, 409–431.
Yildiz, I., Shukla, S., Steinmetz, N.F., 2011. Applications of viral nanoparticles in medicine. Curr. Opin. Biotechnol. 22 (6), 901–908.
Chianese, S., Iovino, P., Leone, V., Musmarra, D., Prisciandaro, M., 2017. Photodegradation of diclofenac sodium salt in water solution: effect of HA, NO 3− and TiO 2 on photolysis performance. Water Air Soil Pollut. 228 (8), 270.
Gao, L., Zhou, B., Wang, F., Yuan, R., Chen, H., Han, X., 2020. Effect of dissolved organic matters and inorganic ions on TiO 2 photocatalysis of diclofenac: mechanistic study and degradation pathways. Environ. Sci. Pollut. Res. 27 (2), 2044–2053.
Iovino, P., Chianese, S., Prisciandaro, M., Musmarra, D., 2019. Triclosan photolysis: operating condition study and photo-oxidation pathway. Chem. Eng. J. 377, 121045.
Novakovic, M., Strbac, G., Petrovic, M., Strbac, D., Mihajlovic, I., 2020. Decomposition of pharmaceutical micropollutant–diclofenac by photocatalytic nanopowder mixtures in aqueous media: effect of optimization parameters, identification of intermediates and economic considerations. J. Environ. Sci. Health Part A 55 (4), 483–497.
Sreedevi, T., Joseph, J., Devi, D.R., Hari, B.V., 2012. Isolation and characterization of lecithin from emu egg as novel pharmaceutical excipient. Rasāyan J. Chem. 5 (3), 414–419.
Sobeih, M.M., El-Shahat, M., Osman, A., Zaid, M., Nassar, M.Y., 2020. Glauconite clay-functionalized chitosan nanocomposites for efficient adsorptive removal of fluoride ions from polluted aqueous solutions. RSC Adv. 10 (43), 25567–25585.
El-Berry, M.F., Sadeek, S.A., Abdalla, A.M., Nassar, M.Y., 2020. Microwave-assisted fabrication of copper nanoparticles utilizing different counter ions: an efficient photocatalyst for photocatalytic degradation of safranin dye from aqueous media. Mater. Res. Bull. 111048.
Li, F.H., Yao, K., Lv, W.Y., Liu, G.G., Chen, P., Huang, H.P., et al, 2015. Photodegradation of ibuprofen under UV–vis irradiation: mechanism and toxicity of photolysis products. Bullet. Environ. Contaminat. Toxicol. 94 (4), 479–483.
Gu, Y., Yperman, J., Carleer, R., D'Haen, J., Maggen, J., Vanderheyden, S., et al, 2019. Adsorption and photocatalytic removal of Ibuprofen by activated carbon impregnated with TiO2 by UV–Vis monitoring. Chemosphere 217, 724–731.
Khan, M., Fung, C.S., Kumar, A., Lo, I.M., 2019. Magnetically separable BiOBr/Fe3O4@ SiO2 for visible-light-driven photocatalytic degradation of ibuprofen: Mechanistic investigation and prototype development. J. Hazard. Mater. 365, 733–743.
Liu, N., Huang, W., Tang, M., Yin, C., Gao, B., Li, Z., et al, 2019. In-situ fabrication of needle-shaped MIL-53 (Fe) with 1T-MoS2 and study on its enhanced photocatalytic mechanism of ibuprofen. Chem. Eng. J. 359, 254–264.
Su, H., Sun, F., Jia, J., He, H., Wang, A., Zhu, G., 2015. A highly porous medical metal–organic framework constructed from bioactive curcumin. Chem. Commun. 51 (26), 5774–5777.
Erucar, I., Keskin, S., 2015. Computational Modeling of bio-MOFs for CO2/CH4 separations. Chem. Eng. Sci. 130, 120–128.
Abazari, R., Mahjoub, A.R., Molaie, S., Ghaffarifar, F., Ghasemi, E., Slawin, A.M.Z., et al, 2018. The effect of different parameters under ultrasound irradiation for synthesis of new nanostructured Fe3O4@bio-MOF as an efficient anti-leishmanial in vitro and in vivo conditions. Ultrason. Sonochem. 43, 248–261.
Sattar, T., Athar, M., 2018. Nano bio-MOFs: Showing drugs storage property among their multifunctional properties. AIMS Mater. Sci. 5 (3), 508–518.
Sattar, T., Athar, M., 2017. Hydrothermal synthesis and characterization of copper glycinate (Bio-MOF-29) and its in vitro drugs adsorption studies. Open J. Inorg. Chem. 7 (02), 17.